Nonlinear Analysis: Hybrid Systems 41 (2021) 101039

Contents lists available at ScienceDirect

Nonlinear Analysis: Hybrid Systems

journal homepage: www.elsevier.com/locate/nahs

Time-triggered and event-triggered control of switched affine systems via a hybrid dynamical approach

Carolina Albea [a,b,*], Alexandre Seuret [b]

[a] Universidad de Sevilla, Department of System Engineering and Automatic Control, Avd. de los Descubrimientos s/n, 41092, Seville, Spain
[b] LAAS-CNRS, Université de Toulouse, CNRS, UPS, 7 avenue du Colonel Roche, 31031 Toulouse, France

ARTICLE INFO

Article history:
Received 28 October 2019
Received in revised form 21 February 2021
Accepted 3 March 2021
Available online 16 March 2021

Keywords:
Switched affine systems
Periodic time-triggered control
Aperiodic event-triggered control
Hybrid dynamical systems
Lyapunov stability
Dwell time

ABSTRACT

This paper focuses on the design of both periodic time- and event-triggered control laws of switched affine systems using a hybrid dynamical system approach. The novelties of this paper rely on the hybrid dynamical representation of this class of systems and on a free-matrix min-projection control, which relaxes the structure of the usual Lyapunov matrix-based min-projection control. This contribution also presents an extension of the usual periodic time-triggered implementation to the event-triggered one, where the control input updates are permitted only when a particular event is detected. Together with the definition of an appropriate optimization problem, a stabilization result is formulated to ensure the uniform global asymptotic stability of an attractor for both types of controllers, which is a neighborhood of the desired operating point. Finally, the proposed method is evaluated through a numerical example.

1. Introduction

Switched affine systems [1] are encountered in many applications including DC-DC power conversion [2,3], biochemical networks [4], aerospace [5] and urban traffic [6]. This class of systems is characterized by the fact that the origin is not necessarily a common equilibrium of all operating modes. This usually prevents from the asymptotic stabilization to this common equilibrium. Indeed, the set of operating points are given by a dynamic averaging, obtaining solutions in the generalized sense of Krasovskii. Many papers can be found in the literature on controlling continuous-time switched affine systems. This is usually achieved thanks to the Lyapunov matrix-based min-projection control strategy [7,8] and several contributions succeeded in applying this strategy to the control of DC-DC power converters [9,10] and even comprising experimental results [11,12]. Moreover, this Lyapunov-based controller was also applied to a more general class of nonlinear switched systems [13].

It is worth noting that this control strategy suffers from a major drawback in continuous time. Indeed, it may lead to arbitrarily fast switching control signals, generating eventually Zeno solutions. Therefore, several contributions aimed at ensuring a minimum dwell-time solution with an admissible chattering around the operating point. To cite only the ones focusing on power converters, the authors of [14] imposed a minimum dwell time, thanks to a time regularization. The solution presented in [3] focused on the specific classical boost converter and [15] does not provide a stability proof. Likewise, the authors of [16] have provided a solution to the control of switched affine systems that avoids Zeno behavior

* Corresponding author at: Universidad de Sevilla, Department of System Engineering and Automatic Control, Avd. de los Descubrimientos s/n, 41092, Seville, Spain.
E-mail address: albea@us.es (C. Albea).

https://doi.org/10.1016/j.nahs.2021.101039
1751-570X/

using both time- and space-regularization and a hybrid dynamical system formulation. Moreover, extended formulations of these systems using a nonlinear systems approach have been considered in [17,18].

In many occasions, the control law has to be implemented periodically in a time-triggered method, as it is generally encountered in electronics [19,20]. Moreover, this periodic implementation constraint also represents a challenge in other fields, as in aerospace [21] or in robotic [22,23]. In order to deal with this issue, a solution consisting in the discretization of a continuous-time model gathering the fact that the control law is periodically updated was provided in [24–26]. However, these results disregard the trajectories between two sampling instants, preventing to provide a complete analysis of the continuous trajectories of the system. Compared to the continuous-time approach, the discrete one has the advantage to disregard the problem of Zeno behavior since it inherently includes a dwell time constraint.

Switched affine systems have been considered often in the literature via the hybrid dynamical paradigm given in [27]. The readers may refer to [3,9,28] for instance. The advantages of this framework rely on the possibility to account for the full continuous/discrete nature of such a class of systems. More especially, it allows to represent in a consistent and elegant manner periodic as well as aperiodic controllers. Hence, this direction can be beneficial for deriving a unified approach to cope with the time- and event-triggered switching control laws as for sampled-data systems. Indeed, several hybrid dynamical models have been considered to capture the particular class of sampled-data systems as explained for instance in [27], and have led to many relevant results as detailed in [29]. This represents the main motivation of this paper, i.e. to enhance a hybrid controller for switched affine systems.

In the present paper, we follow the hybrid dynamical system paradigm provided in [27], generating both a periodic time-triggered control and an aperiodic event-triggered control for switched affine systems, without being based on a Lyapunov matrix-based min-projection control strategy. We first provide a hybrid dynamical model of a controlled switching affine system, whose control input is required to be periodically updated, in the sense that the control input can be only modified at periodic sampling instants, driving to a periodic time-triggered controller. Then, we formulate an optimal control design problem expressed as a set of tractable matrix inequality conditions. The periodic time-triggered control law presents a simple structure, which is based on a so-called free-matrix based control law and which differs from the well-known Lyapunov matrix-based min-projection control [9,25,30] used in this class of systems. This solution also provides a compact attractor of small size, which is proven to be Uniformly Globally Asymptotically Stable (UGAS). This ensures that a given operating point is uniformly globally practically stable. In a second step, the previous model is extended to derive an aperiodic event-triggered control law, which includes a minimum dwell-time constraint. This new hybrid dynamical model allows the controller to keep the same control action while no event are generated after a prescribed dwell time. A numerical example illustrates our contribution and shows the efficiency of our approach in the time- and event-triggered cases.

The paper is organized as follow. The problem formulation is stated in Section 2. The hybrid dynamical model for a time-triggered control is presented in Section 3, proposing a control design, by formulating an optimization problem. Moreover, the extension to an event-triggered control strategy is given in Section 4. In Section 5 some numerical results illustrates the theoretical results. The paper ends with a conclusion section and draws some perspectives.

Notations: Throughout the paper, $\mathbb{N}$ denotes the set of natural numbers, $\mathbb{R}$, the real numbers, $\mathbb{R}_{\geq 0}$ real positive numbers, $\mathbb{R}^n$ the n-dimensional Euclidean space and $\mathbb{R}^{n\times m}$ the set of all real $n \times m$ matrices. The set composed by the first K positive integers, namely $\{1, 2, \ldots, K\}$, is denoted by $\mathbb{K}$. For any n and m in $\mathbb{N}$, matrices I_n and $0_{n,m}$ denote the identity matrix of $\mathbb{R}^{n\times n}$ and the null matrix of $\mathbb{R}^{n\times m}$, respectively. When no confusion is possible, the subscript of these matrices that precises their dimension will be omitted. For any matrix M of $\mathbb{R}^{n\times n}$, the notation $M \succ 0$, ($M \prec 0$) means that M is symmetric positive (negative) definite and $\det(M)$ represents its determinant. Finally, we define Λ as the subset of $[0, 1]^{\mathrm{Card}(\mathbb{K})}$ such that an element λ in Λ has its components, λ_i in $[0, 1]$ for all $i \in \mathbb{K}$ and verifies $\sum_{i\in\mathbb{K}} \lambda_i = 1$.

2. Problem formulation

2.1. System data

Consider the switched affine system governed by the following dynamics:

$$\begin{array}{ll} \dot{z}(t) & = A_{\sigma(t)}z(t) + \mathcal{B}_{\sigma(t)}, \\ \sigma(t) & \in \mathbb{K}, \qquad\qquad \forall t \geq 0 \end{array} \tag{1}$$

where $z(t) \in \mathbb{R}^n$ is the system state, and A_i and $\mathcal{B}_i$ are matrices of appropriate dimensions, for all i in $\mathbb{K}$. The control input is the switching signal $\sigma(t)$ in $\mathbb{K}$. The two following assumptions on the implementation of the control law will be considered in the sequel:

Assumption 1 (*Periodic Time-triggered Control*)**.** There exists a sampling period $T > 0$ and an initial time t_0 (without loss of generality, we will take the convention $t_0 = 0$) such that the switching control input verifies

$$\begin{cases} \sigma(t) = \sigma(t_k), & \forall t \in [t_k,\ t_{k+1}), \\ t_{k+1} = t_k + T, \end{cases} \qquad \forall k \in \mathbb{N}. \tag{2}$$

Assumption 2 (*Aperiodic Event-triggered Control*)**.** There exists a minimum and maximum dwell time $0 < T_m < T_M$, a function ϕ and an initial time $t_0 = 0$, such that the switching control input can be described by

$$\begin{cases} \sigma(t) = \sigma(t_k), \quad \forall t \in [t_k,\ t_{k+1}), \\ t_{k+1} = \min\limits_{t\in\mathbb{R}}\{t \in [t_k + T_m, t_k + T_M],\ \phi(\xi) \geq 0\}, \end{cases} \qquad \forall k \in \mathbb{N}, \tag{3}$$

where function ϕ refers to a triggering rule to be defined, generating the events based on the available information, which is denoted here as ξ.

This paper deals with the design of both periodic time-triggered control law and an aperiodic event-triggered control law for the control input $\sigma(t)$, such that the solutions to switched affine system (1) converge globally and asymptotically to a neighborhood of a desired operating point given by $z_e \in \mathbb{R}^N$. As mentioned in the introduction, this desired operating point, z_e, is not necessarily an equilibrium of one or several modes of (1). The following definition and assumption represent a sufficient condition for characterizing some allowable operating points (see [16,25]).

Definition 1. Consider the set Ω_e given by

$$\Omega_e := \left\{z_e \in \mathbb{R}^n,\quad \exists \lambda \in \Lambda,\quad A_\lambda z_e + \mathcal{B}_\lambda = 0\right\} \tag{4}$$

where $A_\lambda := \sum_{i\in\mathbb{K}} \lambda_i A_i$ and $\mathcal{B}_\lambda := \sum_{i\in\mathbb{K}} \lambda_i \mathcal{B}_i$.

Assumption 3. The desired operating point, denoted as z_e in the remainder of the paper and its associated weighting vector, denoted as λ, belongs to Ω_e.

It is worth noting that Ω_e does not contain all the acceptable functioning points as mentioned in [25].

For any vector z_e in Ω_e, we introduce the error variable $x(t) := z(t) - z_e$, where variable z is driven by system (1), giving rise to the following error dynamics

$$\begin{array}{rl} \dot{x}(t) & = A_{\sigma(t_k)}x + B_{\sigma(t_k)}, \\ \sigma(t_k) & \in \mathbb{K}, \end{array} \qquad \forall t \in [t_k,\ t_{k+1}), \quad \forall k \in \mathbb{N}, \tag{5}$$

where matrices B_i stand for $A_i z_e + \mathcal{B}_i$, for all i in $\mathbb{K}$. Thus, from Assumption 3, the λ in Λ implies $B_\lambda = \sum_{i\in\mathbb{K}} \lambda_i B_i = 0$.

2.2. Control objectives

Even with a suitable control law, it is worth noting that systems (1) and (5) do not necessarily converge to z_e and 0, respectively, but to a neighborhood of them. This might be understood as a chattering effect around a sliding surface of a sampled-data sliding mode control law [31]. In the present paper, our objective is to study such systems using a hybrid dynamical system formulation and analysis as developed in [27]. This is given in the following statement:

Problem 1. Consider system (1) with the periodic time-triggered control formulated in Assumption 1 or the event-triggered one mentioned in Assumption 2. For each case, the objectives of this paper are

(P1) To build a well-posed hybrid dynamical model.
(P2) To design a suitable control law, called free-matrix min-projection control.
(P3) To ensure that a neighborhood of the desired operating point z_e in Ω_e is uniformly globally asymptotically stable to the resulting closed-loop system.
(P4) To provide an optimal parametrization of the control law that minimizes the volume of that neighborhood.

Objective *(P1)* remains in expressing switched affine systems with a periodic or an aperiodic implementation, based on the hybrid dynamical system formulation considered in [27]. Contrary to the usual control law employed in the literature, i.e. Lyapunov matrix-based min projection control (see for instance [7,25,30]) our objective *(P2)* is to provide a relaxed structure for the control law inspired from the ones presented in [26,32]. In order to prove the uniform global asymptotic stability of the system to the neighborhood of the operating point, objective *(P3)*, the non smooth hybrid invariance principle from [33] will be used to characterize the neighborhood of the operating point thanks to a Lyapunov function for the hybrid system. Finally, an optimization problem will be formulated to reduce the size of this neighborhood following the problem presented in [25], fulfilling objective *(P4)*. The novelty of this paper then, relies on the appropriate combination of these ingredients, considering time- and event-triggered control implementations.

3. Time-triggered control

3.1. Definition of a hybrid dynamical model

Considering (5), it is reasonable to model this system as a hybrid dynamical system, following the formalism given in [27], wherein continuous-time behavior is gathered in (5) and the discrete-time behavior is given by the jump of the

control input σ from one mode to another one. A timer τ is included in the hybrid model in order to consider the periodic implementation of the control law. Therefore, the overall dynamics are represented as follows:

$$\mathcal{H}: \begin{cases} \begin{bmatrix} \dot{x} \\ \dot{\tau} \\ \dot{\sigma} \end{bmatrix} = f(x,\tau,\sigma) & (x,\tau,\sigma) \in \mathcal{C}, \\ \\ \begin{bmatrix} x^+ \\ \tau^+ \\ \sigma^+ \end{bmatrix} \in G(x,\tau,\sigma) & (x,\tau,\sigma) \in \mathcal{D}, \end{cases} \tag{6}$$

where $\sigma^+ \subset \mathbb{K}$ is the control law to be designed, $\tau \in \mathbb{R}$ is the timer that has to be constrained to live in the interval $[0, T]$. In the previous equation, f and G are (set-valued) maps that capture the continuous time dynamics as well as the switching logic, which are defined as follow:

$$\begin{aligned} f(x,\tau,\sigma) &:= \begin{bmatrix} A_\sigma x + B_\sigma \\ 1 \\ 0 \end{bmatrix} \quad (x,\tau,\sigma) \in \mathbb{H} := \mathbb{R}^n \times [0,T] \times \mathbb{K}, \\ G(x,\tau,\sigma) &:= \begin{bmatrix} x \\ 0 \\ u(x,\tau,\sigma) \end{bmatrix} \quad (x,\tau,\sigma) \in \mathbb{H}, \end{aligned} \tag{7}$$

where the to-be-designed set valued map $u \in \mathbb{K}$ referring to the control law, is assumed to be outer semi-continuous.

The so-called "flow" and "jump" sets $\mathcal{C}$ and $\mathcal{D}$, respectively, are given by

$$\mathcal{C} := \{(x,\tau,\sigma) : x \in \mathbb{R}^n, \tau \in [0,T], \sigma \in \mathbb{K}\}, \tag{8}$$

$$\mathcal{D} := \{(x,\tau,\sigma) : x \in \mathbb{R}^n, \tau = T, \sigma \in \mathbb{K}\}. \tag{9}$$

Note that the state of this hybrid model is composed of the state vector x, corresponding to the original switched affine system; a timer τ that captures the elapsed time since the last control update and, the control input σ selected in the countable and bounded set $\mathbb{K}$. This model captures the whole dynamics of the sampled-data controlled system (see [29] for more details). Indeed, the system is allowed to flow only when $\tau \leq T$, which corresponds to the differential equation given by the map $f(x,\tau,\sigma)$ in $\mathcal{H}$. Note that x evolves following the affine dynamic, timer τ increases as the time and the control input σ remains constant.

Likewise, the system is allowed to jump only when $\tau = T$, which corresponds to an update of the sampled-data switching control input as described by the jump map G in $\mathcal{H}$. During jumps, vector x remains constant, while timer τ is reset to 0 and, control input σ is allowed to be modified according to the control law $u(x,\tau,\sigma)$.

This hybrid model description of $\mathcal{H}$ presents good structural properties (see Proposition 1 below) and shows a periodic character of the jumps. Based on the previous considerations, the following proposition is stated.

Proposition 1. *System $\mathcal{H}(f, G, \mathcal{C}, \mathcal{D})$ is well-posed.*

Proof 1. Knowing from (6)–(9) that u belongs to $\mathbb{K}$, whose cardinal is bounded, it is easy to see that hybrid system $\mathcal{H}(f, G, \mathcal{C}, \mathcal{D})$ verifies the following properties

- $\mathcal{C}$ and $\mathcal{D}$ are closed sets in $\mathbb{H}$;
- f is a continuous function, thus locally bounded and outer semi-continuous. Moreover, $f(x,\tau,\sigma)$ is obviously convex for each $(x,\tau,\sigma) \in \mathcal{C}$, since $f(x,\tau,\sigma)$ is reduced to a vector of $\mathbb{R}^{n+2}$;
- G is locally bounded and outer semi-continuous.

Therefore, it satisfies the basic hybrid conditions [27, Assumption 6.5] and following [27, Theorem 6.30], we can conclude that it is well posed.

Solutions to $\mathcal{H}(f, G, \mathcal{C}, \mathcal{D})$ are given on the hybrid time domain: $\mathrm{dom}(x,\tau,\sigma) \subset \mathbb{R}_{\geq 0} \times \mathbb{N}$, such that

$$\mathrm{dom}(x,\tau,\sigma) = \bigcup_{k=0}^{\bar{k}-1} ([t_k, t_{k+1}], k), \tag{10}$$

with $\bar{k}$ finite (being $\mathrm{dom}(x,\tau,\sigma)$ a compact hybrid time domain) or infinite.

It is readily seen from system (5) that the following expression holds

$$\begin{bmatrix} \dot{x} \\ 0 \end{bmatrix} = \Gamma_\sigma \begin{bmatrix} x \\ 1 \end{bmatrix}, \quad \text{with} \quad \Gamma_\sigma := \begin{bmatrix} A_\sigma & B_\sigma \\ 0_{1,n} & 0 \end{bmatrix}, \tag{11}$$

so that the so-called hybrid arc (hybrid inclusion in [27]) defined in $I^k = [t_k, t_{k+1}]$ are given by

$$\begin{bmatrix} x_{k+1} \\ 1 \end{bmatrix} = e^{\Gamma_\sigma T} \begin{bmatrix} x_k \\ 1 \end{bmatrix}. \tag{12}$$

In the sequel, we will characterize some particular hybrid arcs that reach the origin just after a jump.

Definition 2. Let us introduce the following set of hybrid arcs, defined as follows:

$$\mathcal{E} = \left\{ (x, \tau, \sigma) \in \mathbb{H} \mid x = \begin{bmatrix} I & 0 \end{bmatrix} e^{\Gamma_\sigma \tau} \begin{bmatrix} 0 \\ 1 \end{bmatrix} \right\}. \tag{13}$$

In order to better understand the main motivation to introduce this set, let us note that, if $\tau = 0$, it is straightforward to see that the corresponding x is equal to zero. Hence, $x = \begin{bmatrix} I & 0 \end{bmatrix} e^{\Gamma_\sigma \tau} \begin{bmatrix} 0 \\ 1 \end{bmatrix}$ describes a solution that crosses the origin $(x, \tau, \sigma) = (0, 0, \sigma)$ and flows from this point.

3.2. Definition of the attractor for time-triggered control

When considering system (5) with a T-periodic sampled-data control implementation of the input variable, σ, asymptotic stability to zero is in general not possible. However, only a practical stabilization of an operating point $x_e \in \Omega_e$ can be achieved. This can be also characterized by the asymptotic stability to a neighborhood of the origin. In this paper, we will consider this second formulation, where the attractor set will be defined through an appropriate candidate Lyapunov function, which is expressed using a positive definite matrix P to be defined latter on and is given by

$$V(x, \tau, \sigma) = \max \{ W(x, \tau, \sigma) - 1, 0 \}, \tag{14}$$

where W is a quadratic function of x, such that

$$W(x, \tau, \sigma) \quad := \quad \begin{bmatrix} x \\ 1 \end{bmatrix}^\top \mathcal{P}(\tau, \sigma) \begin{bmatrix} x \\ 1 \end{bmatrix}. \tag{15}$$

The function $\mathcal{P}$ is a matrix depending on the timer τ and on the active mode, σ. Several ways of constructing such timer-dependent functions have already been considered and the readers may refer to [34] to see some other examples. In this paper, we want to extend the formulation provided in [27] for periodic sampled-data control systems. This corresponds to the following definition

$$\begin{aligned} \mathcal{P}(\tau, \sigma) &= e^{-\Gamma_\sigma^\top \tau} \begin{bmatrix} P & h \\ h^\top & h^\top P^{-1} h \end{bmatrix} e^{-\Gamma_\sigma \tau} \\ &= e^{-\Gamma_\sigma^\top \tau} \begin{bmatrix} P \\ h^\top \end{bmatrix} P^{-1} \begin{bmatrix} P & h \end{bmatrix} e^{-\Gamma_\sigma \tau}, \end{aligned} \tag{16}$$

where matrices Γ_i, $i \in \mathbb{K}$ has been defined in (11). From the last expression, it is clear that the positive definiteness of P ensures in the previous expression that $\mathcal{P}$ is positive semi-definite and h is a vector that allows to shift the center of the level set, i.e. $\begin{bmatrix} x \\ 1 \end{bmatrix}^\top \mathcal{P}(\tau, \sigma) \begin{bmatrix} x \\ 1 \end{bmatrix} \geq 0$, for any $x \in \mathbb{R}$. We are now in position to define the compact attractor, which is characterized as follows:

$$\mathcal{A} := \{ (x, \tau, \sigma) \in \mathcal{C} \cup \mathcal{D} \quad V(x, \tau, \sigma) = 0 \}. \tag{17}$$

This attractor refers to the elements of $\mathbb{H}$, that verify $W(x, \tau, \sigma) \leq 1$. It is worth noting that this set is described in an extended space composed not only by the system state x, but also by the timer τ and the active mode σ.

It is easy to see that V is continuous in $\mathcal{C} \cup \mathcal{D}$ and locally Lipschitz near each point in $\mathcal{C} \backslash \mathcal{A}$. Moreover, V is positive definite with respect to $\mathcal{A}$ in $\mathcal{C} \cup \mathcal{D}$ and radially unbounded.

Note that the minimum of W with respect to x is not necessarily reached when (x, τ, σ) is equal to $(0, 0, \sigma)$. This is due to the introduction of parameter h, which allows shifting this minimum to another location. In order to achieve the control objectives, which means that the solutions are ensured to converge to a neighborhood of the origin, one has to guarantee that $(0, 0, \sigma)$ belongs to $\mathcal{A}$. More generally, regarding the definition of $\mathcal{E}$ in (13), it will be required that $\mathcal{E}$ is included in the attractor $\mathcal{A}$, to state that the origin is in the interior of the attractor.

Remark 1. Note that function W is a relatively simple quadratic function, whose center is shifted to the position defined by vector h. More involved functions can be found in the literature of switched affine systems, as for instance in [35], where the Lyapunov matrix P is allowed to depend on the active mode. This is not considered in this paper for the sake of simplicity. Indeed, our objective is more focused on the hybrid framework and on the extension to the design of an event-triggered controller developed in the next section. ⌟

3.3. Design of an efficient switching control law

Once the Objective *(P1)* is fulfilled by the hybrid dynamical model given in $\mathcal{H}$, (6), we propose, in this section, a novel stabilization based on a relaxed control law, which notably differs from the classical Lyapunov matrix-based min-projection control developed in [7,25,30], among others. This is stated in the following theorem.

Theorem 1. *For a given z_e in Ω_e and a given $T \in \mathbb{R}_{\geq 0}$, assume that matrices $0 \prec P \in \mathbb{R}^{n\times n}$, $h \in \mathbb{R}^n$, $N_i = N_i^\top \in \mathbb{R}^{(n+1)\times(n+1)}$, for all $i \in \mathbb{K}$ and parameter $0 < \mu < 1$ are the solution to the optimization problem*

$$\min_{P,h,N_i,\mu} \quad -\log(\det(P)), \tag{18}$$

$$s.t.\ P \succ 0, \tag{19}$$

$$\Phi_i(T) = \begin{bmatrix} \Psi_i(T) + N_\lambda - N_i - \begin{bmatrix} 0 & 0 \\ * & \mu \end{bmatrix} & \mu \begin{bmatrix} P \\ h^\top \end{bmatrix} \\ * & -\mu P \end{bmatrix} \prec 0, \qquad \forall i \in \mathbb{K}, \tag{20}$$

$$\Theta_\lambda(T) = \begin{bmatrix} 0 \\ 1 \end{bmatrix}^\top \Psi_\lambda(T) \begin{bmatrix} 0 \\ 1 \end{bmatrix} \succeq 0, \tag{21}$$

where $\lambda \in \Lambda$ is related to z_e satisfying Assumption 3 and

$$\Psi_i(T) := e^{\Gamma_i^\top T} \begin{bmatrix} P & h \\ h^\top & 0 \end{bmatrix} e^{\Gamma_i T} - \begin{bmatrix} P & h \\ h^\top & 0 \end{bmatrix}. \tag{22}$$

$$N_\lambda := \sum_{i\in\mathbb{K}} \lambda_i N_i \quad \text{and} \quad \Psi_\lambda(T) := \sum_{i\in\mathbb{K}} \lambda_i \Psi_i(T).$$

Then, the following control law, given by

$$u(x,\tau,\sigma) \in \underset{j\in\mathbb{K}}{argmin} \begin{bmatrix} x \\ 1 \end{bmatrix}^\top N_j \begin{bmatrix} x \\ 1 \end{bmatrix} \tag{23}$$

with $x := z - z_e$ ensures that map G is locally bounded and outer semi-continuous the following statements hold for hybrid system (6):

(i) *$\mathcal{A}$ defined in (17) is UGAS and*

(ii) *$\mathcal{E}$ defined in (13) is included in $\mathcal{A}$.* □

Remark 2. The optimization problem given in Theorem 1 is subject to a bilinear matrix inequality, which is known to be non-convex. However, the problem can be easily avoided by performing a line-search routine for $\mu \in (0, 1)$ and by noting that the resulting problem has become linear with respect to the decision variables. Note that this procedure was already adopted in [25]. ⌟

Proof 2. For a given sampling period, T, let us consider a solution to the optimization described in Theorem 1. That is parameter $\mu \in (0, 1)$ and matrices $P \succ 0 \in \mathbb{R}^{n\times n}$, $h \in \mathbb{R}^n$, $N_i = N_i^\top \in \mathbb{R}^{(n+1)\times(n+1)}$ with $i \in \mathbb{K}$ verify problem (18)–(21). In the sequel, the proof of items (i) and (ii) will be considered successively.

Proof of (i): The proof of item (i) relies on the application of [33, Theorem 1]. First, note that the candidate Lyapunov function, V (14) is locally Lipschitz, radially unbounded and verifies, by definition $V(x,\tau,\sigma) = 0$, for all (x,τ,σ) in $\mathcal{A}$ and strictly positive otherwise as shown in Eq. (16), where matrix P is assumed to be positive definite.

The next step of the proof is to ensure that the derivative of V along flows outside of $\mathcal{A}$ is non positive (or more precisely in this case, equal to zero). More formally, the objective is to show

$$\langle \nabla V(x,\tau,\sigma), f(x,\sigma)\rangle \leq 0, \quad \forall (x,\tau,\sigma) \in \mathcal{C}\backslash\mathcal{A}. \tag{24}$$

For any $(x,\tau,\sigma) \in \mathcal{C}\backslash\mathcal{A}$, it is clear, from its definition, that $V(x,\tau,\sigma) = W(x,\tau,\sigma) - 1$ and we get that

$$\begin{aligned} \langle \nabla V(x,\tau,\sigma), f(x,\sigma)\rangle &= \begin{bmatrix} x \\ 1 \end{bmatrix}^\top \left(\dot\tau \tfrac{\partial}{\partial\tau}\mathcal{P}(\tau,\sigma) + \dot\sigma \tfrac{\partial}{\partial\sigma}\mathcal{P}(\tau,\sigma)\right) \begin{bmatrix} x \\ 1 \end{bmatrix} + 2 \begin{bmatrix} x \\ 1 \end{bmatrix}^\top \mathcal{P}(\tau,\sigma) \begin{bmatrix} \dot x \\ 0 \end{bmatrix} \\ &= \begin{bmatrix} x \\ 1 \end{bmatrix}^\top \left(\tfrac{\partial}{\partial\tau}\mathcal{P}(\tau,\sigma) + \mathrm{He}\left(\mathcal{P}(\tau,\sigma)\Gamma_\sigma\right)\right) \begin{bmatrix} x \\ 1 \end{bmatrix} = 0, \end{aligned}$$

which is guaranteed by the construction of $\mathcal{P}$ in (16), and ensures condition (24). Note the second stability condition from [33, Theorem 1], that is

$$\Delta V(x,\tau,\sigma) := \max_{g\in G(x,\tau,\sigma)\cap(\mathcal{C}\cup\mathcal{D})} V(g) - V(x,\tau,\sigma) < 0, \quad \forall (x,\tau,\sigma) \in \mathcal{D}\setminus\mathcal{A}. \tag{25}$$

Again, consider any (x,τ,σ) in $\mathcal{D}\backslash\mathcal{A}$, such that $V(x,\tau,\sigma)=W(x,\tau,\sigma)-1$ and any g in $G(x,\tau,\sigma)\cap(\mathcal{C}\cup\mathcal{D})$. Since (x,τ,σ) is in $\mathcal{D}\backslash\mathcal{A}$, then $\tau=T$. Moreover, since g is in $G(x,\tau,\sigma)\cap(\mathcal{C}\cup\mathcal{D})$, then $g=(x,0,\sigma^+)$ where σ^+ belongs to $u(x)$. If $(x,0,\sigma^+)$ belongs to $\mathcal{A}$, then $V(x,0,\sigma^+)-V(x,T,\sigma)=-V(x,T,\sigma)<0$. Otherwise we have

$$\begin{aligned}V(x,0,\sigma^+)-V(x,T,\sigma) &= W(x^+,0,\sigma^+)-W(x,T,\sigma)\\ &=\begin{bmatrix}x\\1\end{bmatrix}^\top\left(\mathcal{P}(0,\sigma^+)-\mathcal{P}(T,\sigma)\right)\begin{bmatrix}x\\1\end{bmatrix}\\ &=\begin{bmatrix}x\\1\end{bmatrix}^\top\left(\begin{bmatrix}P & h\\ h^\top & h^\top P^{-1}h\end{bmatrix}-e^{-\Gamma_\sigma^\top T}\begin{bmatrix}P & h\\ h^\top & h^\top P^{-1}h\end{bmatrix}e^{-\Gamma_\sigma T}\right)\begin{bmatrix}x\\1\end{bmatrix}\\ &=\begin{bmatrix}x\\1\end{bmatrix}^\top\left(\begin{bmatrix}P & h\\ h^\top & 0\end{bmatrix}-e^{-\Gamma_\sigma^\top T}\begin{bmatrix}P & h\\ h^\top & 0\end{bmatrix}e^{-\Gamma_\sigma T}\right)\begin{bmatrix}x\\1\end{bmatrix}.\end{aligned}$$

This last simplification comes from the fact that the last diagonal component of $e^{-\Gamma_\sigma T}$ is 1. Therefore, we can express the previous equation thanks to the matrices Ψ_i's defined in (22) as follows

$$V(x,0,\sigma^+)-V(x,T,\sigma)=\left(e^{-\Gamma_\sigma T}\begin{bmatrix}x\\1\end{bmatrix}\right)^\top\Psi_\sigma(T)\left(e^{-\Gamma_\sigma T}\begin{bmatrix}x\\1\end{bmatrix}\right). \tag{26}$$

For the sake of simplicity, we will use the following notation along the proof,

$$\begin{bmatrix}\chi_\sigma\\1\end{bmatrix}=e^{-\Gamma_\sigma T}\begin{bmatrix}x\\1\end{bmatrix}. \tag{27}$$

Notice that, in this definition, vector χ_σ depends on the state x, on the sampling period T and on the active mode σ. This dependence is not specified in this notation to avoid heavy notations. In order to better emphasize the link between x and χ_σ stated in (27), let us rewrite this statement in the usual discrete-time framework. In this equation, we would write $x=x(k+1)$ and $\chi_\sigma=x(k)$. The dynamics leading to $x(k+1)$ from $x(k)$ is driven by $\left[\begin{smallmatrix}x(k+1)\\1\end{smallmatrix}\right]=e^{\Gamma_\sigma T}\left[\begin{smallmatrix}x(k)\\1\end{smallmatrix}\right]$, which result from the integration of the differential (flow) equation over a sampling interval of length T.

We also note that this new notation is of high importance since it corresponds to the state of the switched affine system just after the jump. Hence, according to (12), this can be formalized as follows

$$\sigma\in\operatorname*{argmin}_{j\in\mathbb{K}}\begin{bmatrix}\chi_\sigma\\1\end{bmatrix}^\top N_j\begin{bmatrix}\chi_\sigma\\1\end{bmatrix}.$$

This implies that inequalities

$$\begin{bmatrix}\chi_\sigma\\1\end{bmatrix}^\top(N_j-N_\sigma)\begin{bmatrix}\chi_\sigma\\1\end{bmatrix}\geq 0,$$

hold for any $j\in\mathbb{K}$. Therefore, for any convex combination, and more particularly for λ in Λ, we have

$$\Sigma_\sigma(x,T,\sigma):=\begin{bmatrix}\chi_\sigma\\1\end{bmatrix}^\top(N_\lambda-N_\sigma)\begin{bmatrix}\chi_\sigma\\1\end{bmatrix}\geq 0. \tag{28}$$

The previous expression allows to introduce the condition that σ is the active node. Let us now specify that (x,T,σ) is in $\mathcal{D}\backslash\mathcal{A}$. From the definition of $\mathcal{A}$, this means that $V(x,T,\sigma)>0$ and

$$\begin{aligned}0<W(x,T,\sigma)-1 &=\begin{bmatrix}x\\1\end{bmatrix}^\top\mathcal{P}(T,\sigma)\begin{bmatrix}x\\1\end{bmatrix}-1\\ &=\begin{bmatrix}\chi_\sigma\\1\end{bmatrix}^\top\begin{bmatrix}P & h\\ h^\top & h^\top P^{-1}h-1\end{bmatrix}\begin{bmatrix}\chi_\sigma\\1\end{bmatrix},\end{aligned}$$

where we have employed (27) to enforce the use of notation χ_σ. Therefore, (25) is verified, if we can prove that inequality

$$\begin{bmatrix}\chi_\sigma\\1\end{bmatrix}^\top\Psi_\sigma(T)\begin{bmatrix}\chi_\sigma\\1\end{bmatrix}<0$$

holds for all (x,τ,σ) in $\mathcal{D}\backslash\mathcal{A}$ such that

$$\begin{bmatrix}\chi_\sigma\\1\end{bmatrix}^\top\begin{bmatrix}P & h\\ h^\top & h^\top P^{-1}h-1\end{bmatrix}\begin{bmatrix}\chi_\sigma\\1\end{bmatrix}\geq 0$$

$$\text{and}\quad\begin{bmatrix}\chi_\sigma\\1\end{bmatrix}^\top(N_\lambda-N_\sigma)\begin{bmatrix}\chi_\sigma\\1\end{bmatrix}^\top\geq 0,$$

where we recall that vector χ_σ, defined in (27), depends explicitly on (x, τ, σ). Using two successive S-procedures, this problem is recast into the existence of a parameter $\mu > 0$, such that,

$$\Psi_i(T) + N_\lambda - N_i + \mu \begin{bmatrix} P & h \\ h^\top & h^\top P^{-1} h - 1 \end{bmatrix} \prec 0, \quad i \in \mathbb{K}. \tag{29}$$

By noting that matrix $\left[\begin{smallmatrix} P & h \\ h^\top & h^\top P^{-1} h \end{smallmatrix}\right]$ can be rewritten as $\left[\begin{smallmatrix} P \\ h^\top \end{smallmatrix}\right] P^{-1} \left[\begin{smallmatrix} P \\ h^\top \end{smallmatrix}\right]^\top$, such that the application of the Schur complement to this term leads to condition (20). It can then, be concluded that if (20) is satisfied, then condition (25) is also verified.

In order to complete the proof, the assumption of [33, Theorem 1], consisting in the satisfaction of $G(\mathcal{A} \cap \mathcal{D}) \subset \mathcal{A}$ has to be included. This condition consists in proving that $\mathcal{A}$ is invariant. Let us first note that in the proof of (24), we prove that V is constant in $\mathcal{C} \cap \mathcal{A}$. Then, let us consider (x, τ, σ) in $\mathcal{D} \cap \mathcal{A}$. We have seen in the previous calculations that inequality (20) yields

$$\begin{aligned} &\left(e^{-\Gamma_\sigma T} \begin{bmatrix} x \\ 1 \end{bmatrix}\right)^\top \left(\Psi_i(T) + N_\lambda - N_i + \mu \begin{bmatrix} P & h \\ h^\top & h^\top P^{-1} h - 1 \end{bmatrix}\right) \left(e^{-\Gamma_\sigma T} \begin{bmatrix} x \\ 1 \end{bmatrix}\right) \\ &\quad = W(x, 0, \sigma^+) - W(x, T, \sigma) + \mu(W(x, T, \sigma) - 1) + \Sigma_\sigma < 0, \end{aligned}$$

where Σ_σ is defined in (28) and is a positive quantity. Hence, the previous expression can be rewritten as follows

$$W(x, 0, \sigma^+) - 1 < (1 - \mu)(W(x, T, \sigma) - 1) - \Sigma_\sigma \leq (1 - \mu)(W(x, T, \sigma) - 1).$$

Therefore, since $\mu \in (0, 1)$ and $(x, T, \sigma) \in \mathcal{A}$, ensures that $W(x, 0, \sigma^+) - 1$ is negative, such that, $V(x, 0, \sigma^+)$ is zero, which was to be proven. The last step of the proof is to ensure that no complete solution, that are not in $\mathcal{A}$, keeps constant, this means that there is no complete solution such that

$$V(x(t, j), \tau(t, j), \sigma(t, j)) = V(x(0, 0), \tau(0, 0), \sigma(0, 0)) \neq 0,$$

for all $(t, j) \in \mathrm{dom}(x, \tau, \sigma)$. This is ensured by the facts that condition (20) is a strict inequality and that jumps are forced to occurs after T ordinary time. Therefore, by application of [33, Theorem 1], attractor $\mathcal{A}$ is UGAS for hybrid system $\mathcal{H}$.

Proof of (ii): The objective here is to prove that the particular solutions in $\mathcal{E}$ are in the interior of $\mathcal{A}$. Recall that $\mathcal{E}$ contains the solutions that reach the origin (in x) right after a jump. Formally, this means that inequality

$$\left(e^{\Gamma_\sigma \tau} \begin{bmatrix} 0 \\ 1 \end{bmatrix}\right)^\top \mathcal{P}(\tau, \sigma) \left(e^{\Gamma_\sigma \tau} \begin{bmatrix} 0 \\ 1 \end{bmatrix}\right) = \begin{bmatrix} 0 \\ 1 \end{bmatrix}^\top \mathcal{P}(0, \sigma) \begin{bmatrix} 0 \\ 1 \end{bmatrix} = h^\top P^{-1} h \leq 1,$$

holds for any (τ, σ) in $[0, T] \times \mathbb{K}$. To proceed with this proof, let us compute the linear combination of (29) (which is equivalent to (20)), weighted by λ. This yields

$$\sum_{i \in \mathbb{K}} \lambda_i \left(\Psi_i(T) + N_\lambda - N_i + \mu \begin{bmatrix} P & h \\ h^\top & h^\top P^{-1} h - 1 \end{bmatrix}\right) \prec 0.$$

Using the condition $\sum_{i \in \mathbb{K}} \lambda_i = 1$ and the fact that $\sum_{i \in \mathbb{K}} \lambda_i N_i = N_\lambda$, the previous inequality leads to

$$\sum_{i \in \mathbb{K}} \lambda_i \Psi_i(T) + \mu \begin{bmatrix} P & h \\ h^\top & h^\top P^{-1} h - 1 \end{bmatrix} \prec 0. \tag{30}$$

Pre- and post-multiplying this inequality by the vector $\left[\begin{smallmatrix} 0 \\ 1 \end{smallmatrix}\right]^\top$ and its transpose, respectively provides

$$\left[\begin{smallmatrix} 0 \\ 1 \end{smallmatrix}\right]^\top \sum_{i \in \mathbb{K}} \lambda_i \Psi_i(T) \left[\begin{smallmatrix} 0 \\ 1 \end{smallmatrix}\right] + \mu(h^\top P^{-1} h - 1) < 0.$$

From condition (21), the first term of the previous inequality is positive. This necessarily implies that $h^\top P^{-1} h - 1$ is negative, which was to be demonstrated.

The hybrid dynamical model given in (6)–(7) together with the solution of the optimization problem given in Theorem 1 satisfy all items of Problem 1.

The previous theorem presents a constructive stabilization result for sampled-data switched affine systems, which depends explicitly on the value of the sampling period T. Then, the influence of T on the feasibility of (20)–(21) needs to be studied carefully. To do so, the two following propositions are stated to better understand the underlying necessary conditions for their feasibility.

Proposition 2. *For a given T, a necessary condition for the feasibility of the conditions of Theorem 1 is that there exists a weighting vector $\lambda \in \Lambda$ such that matrix $\sum_{i \in \mathbb{K}} \lambda_i e^{A_i T}$ is Schur stable.*

Proof 3. Following the procedure of Proposition 1 in [26], multiplying inequality (30) by matrix $\left[\begin{smallmatrix} I \\ 0 \end{smallmatrix}\right]$ from the right side and its transpose from the left, leads to $\sum_{i \in \mathbb{K}} \lambda_i e^{A_i^\top T} P e^{A_i T} - (1 - \mu) P < 0$. Since μ belongs to $(0, 1)$, a convexity argument ensures matrix $\sum_{i \in \mathbb{K}} \lambda_i e^{A_i T}$ must be Schur stable.

Proposition 3. *If there exist a weighting vector $\lambda \in \Lambda$ such that $A_\lambda = \sum_{i\in\mathbb{K}} \lambda_i A_i$ is Hurwitz stable, then there exists a sufficiently small sampling period T such that the conditions of Theorem 1 are verified. Moreover, attractor $\mathcal{A}$ tends to $\{-A_\lambda^{-1}B_\lambda\}$ as T tends to zero.*

Proof 4. Consider again inequality (30) in the situation when T is sufficiently small. Performing the Taylor series of $e^{A_i T}$ as T tends to 0, and pre-(and post-) multiplying the result by $\begin{bmatrix} P^{-1} & -P^{-1}h \\ 0 & 1 \end{bmatrix}^\top$ (by its transpose), we obtain

$$\begin{bmatrix} A_\lambda P^{-1} + P^{-1}A_\lambda^\top + \frac{\mu}{T}P^{-1} + \mathrm{O}(T) & A_\lambda P^{-1}h + B_\lambda + \mathrm{O}(T) \\ * & -\frac{\mu}{T} \end{bmatrix} \prec 0,$$

where notation $\mathrm{O}(T)$ stands for a quantity of order T as T tends to 0. Therefore, if there exists a linear combination $\lambda \in \Lambda$ such that matrix A_λ is Hurwitz, then there exist a matrix $P = (\beta W)^{-1}$, with $\beta > 0$, and a sufficiently small $\tilde{\mu} = \mu/T$ such that, for a small value of T,

$$\begin{bmatrix} \beta(A_\lambda W + WA_\lambda^\top + \tilde{\mu}W) + \mathrm{O}(T) & \mathrm{O}(T) \\ * & -\tilde{\mu} \end{bmatrix} \prec 0,$$

because $A_\lambda W + WA_\lambda^\top + \tilde{\mu}W \prec 0$ and $h = -(A_\lambda P^{-1})^{-1}B_\lambda$. Therefore, for a given parameter $\beta > 0$, there exists a sufficiently small value of T such that the necessary conditions given in Theorem 1 are satisfied. Moreover, when T tends to zero, it is possible to select a parameter β, which tends to zero as well, which implies, from its definition, that the Lyapunov matrix, P, becomes large and consequently, that attractor $\mathcal{A}$ shrinks to singleton $\{P^{-1}h\} = \{-A_\lambda^{-1}B_\lambda\}$.

Remark 3. Theorem 1 and the one presented in [26, Theorem 1] address the same problem, but the main difference is that Theorem 1 additionally characterizes the inter-switching dynamics. Even though they provide equivalent stabilization conditions, Theorem 1 is, indeed, dedicated to hybrid dynamical model while results in [26, Theorem 1] only focus on the discrete-time one. ⌟

Remark 4. The optimization problem formulated in Theorem 1 consists in the minimization of a characteristic of attractor $\mathcal{A}$. Indeed, maximizing $\log(\det(P))$ refers to the minimization of the volume of the ellipse defined by the positive definite matrix P. ⌟

4. Event-triggered control

4.1. Definition of a new hybrid dynamical model

In this section, we want to relax the constraint on the periodic update of the switching control law, by considering Assumption 2. This relaxation allows that the trajectories reach a region around a given operating point $z_e \in \Omega_e$ with less control updates than using the periodic-switching control considered in Assumption 1. To do so, let us represent the overall dynamics as follows:

$$\tilde{\mathcal{H}}: \begin{cases} \begin{bmatrix} \dot{x} \\ \dot{\tau} \\ \dot{\sigma} \end{bmatrix} = f(x,\tau,\sigma) & (x,\tau,\sigma) \in \tilde{\mathcal{C}}, \\ \\ \begin{bmatrix} x^+ \\ \tau^+ \\ \sigma^+ \end{bmatrix} \in G(x,\tau,\sigma) & (x,\tau,\sigma) \in \tilde{\mathcal{D}}, \end{cases} \tag{31}$$

where we use the same three components and the same maps f and G to express the state variables as in the periodic time-triggered implementation considered in Section 3.1. However, in order to enforce the event-triggered control, the definition of the jump and flow sets $\tilde{\mathcal{C}}$ and $\tilde{\mathcal{D}}$ have to be modified. Let us first recall maps f and G that capture the new features of the system, as well as, the switching logic. For a sufficiently large positive real T_M, they are now defined as follows:

$$\begin{aligned} f(x,\tau,\sigma) &:= \begin{bmatrix} A_\sigma x + B_\sigma \\ 1 \\ 0 \end{bmatrix} \quad (x,\tau,\sigma) \in \tilde{\mathbb{H}} := \mathbb{R}^n \times [0, T_M] \times \mathbb{K}, \\ G(x,\tau,\sigma) &:= \begin{bmatrix} x \\ 0 \\ u(x,\tau,\sigma) \end{bmatrix} \quad (x,\tau,\sigma) \in \tilde{\mathbb{H}}, \end{aligned} \tag{32}$$

where the to-be-designed set valued map $u \in \mathbb{K}$ referring to the control law, is assumed to be outer semi-continuous.

The timer presents the same role as in the previous section, i.e. keeping track of the elapsed time since the last jump. Timer τ is now enforced to lie in the interval $[0, T_M]$, so that T_M can be seen as a maximum dwell time parameter, which

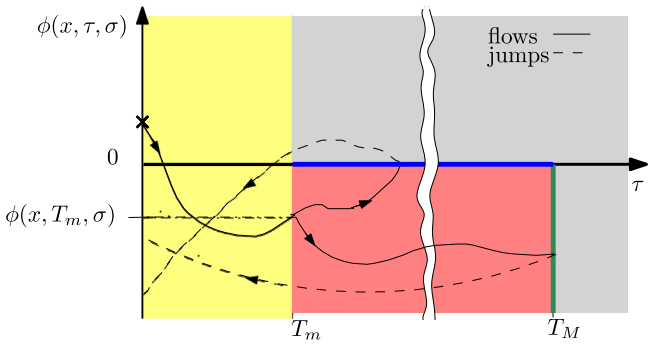

Fig. 1. Illustration in the plan $\tau, \phi(x,\tau,\sigma)$ of the jump set, represented by the blue and green lines and of the flow set by the yellow and red areas. The figure also shows two potential solutions to hybrid system $\tilde{\mathcal{H}}(f, G, \tilde{\mathcal{C}}, \tilde{\mathcal{D}})$, starting from a same point, at $\tau = 0$ and $\phi > 0$. The solid and dashed lines represent the trajectories during flows and jumps, respectively. Moreover, the gray area represents the region where solutions are not allowed to evolve in.

can be selected arbitrarily. Likewise, a minimum dwell time parameter $T_m \in [0,\ T_M]$ has now to be included. The new flow and jump sets $\tilde{\mathcal{C}}$ and $\tilde{\mathcal{D}}$, respectively, are now given by

$$\tilde{\mathcal{C}} := (\mathcal{C}_{T_m} \cup \mathcal{C}_e) \cap \mathcal{C}_{T_M} \tag{33}$$

$$\tilde{\mathcal{D}} := (\mathcal{D}_{T_m} \cap \mathcal{D}_e) \cup \mathcal{D}_{T_M}, \tag{34}$$

where

$$\text{Minimum dwell time} \quad \begin{cases} \mathcal{C}_{T_m} & := \{(x,\tau,\sigma) \in \tilde{\mathbb{H}} : \tau \leq T_m\} \\ \mathcal{D}_{T_m} & := \{(x,\tau,\sigma) \in \tilde{\mathbb{H}} : \tau \geq T_m\}, \end{cases}$$

$$\text{Maximum dwell time} \quad \begin{cases} \mathcal{C}_{T_M} & := \{(x,\tau,\sigma) \in \tilde{\mathbb{H}} : \tau \leq T_M\} \\ \mathcal{D}_{T_M} & := \{(x,\tau,\sigma) \in \tilde{\mathbb{H}} : \tau = T_M\}, \end{cases}$$

$$\text{Event-triggering rule} \quad \begin{cases} \mathcal{C}_e & := \left\{(x,\tau,\sigma) \in \tilde{\mathbb{H}},\ \tau \in [T_m, T_M],\ \phi(x,\tau,\sigma) \leq 0\right\}, \\ \mathcal{D}_e & := \left\{(x,\tau,\sigma) \in \tilde{\mathbb{H}},\ \tau \in [T_m, T_M],\ \phi(x,\tau,\sigma) = 0\right\}, \end{cases}$$

where $\phi : \tilde{\mathbb{H}} \to \mathbb{R}$ is the triggering function, which allows the controller to decide whether or not an event occurs. For the sake of consistency, the definition of this function will be given in the sequel. The following constraint on ϕ is imposed

$$\phi(x, T_m, \sigma) \leq 0, \quad \forall (x,\sigma) \in \mathbb{R}^n \times \mathbb{K}. \tag{35}$$

We also note that some elements of $\tilde{\mathbb{H}}$ are disregarded. Indeed, the element of $\left\{(x,\tau,\sigma) \in \tilde{\mathbb{H}},\ \tau \in [T_m, T_M],\ \phi(x,\tau,\sigma) > 0\right\}$ are not relevant to consider in this study.

Sets $\tilde{\mathcal{C}}$ and $\tilde{\mathcal{D}}$ are subspaces of $\tilde{\mathbb{H}}$. The system has to be understood as follows. According to (33), the system is constrained to flow

- when the timer is lower than the minimum dwell time T_m, as depicted in Fig. 1 by the yellow area.
- when the timer is greater than T_m, and both the triggering condition $\phi(x,\tau,\sigma) \leq 0$ remains satisfied and the timer τ remains lower than the maximum dwell time T_M, as depicted in Fig. 1 by the red area.

Reversely, according to (34), the system is constrained to jump

- when the timer is greater than the minimum dwell time T_m and when $\phi(x,\tau,\sigma) = 0$ becomes true, i.e. the bold blue line in Fig. 1.
- when the timer becomes equal to the maximum dwell time T_M, while the triggering condition $\phi(x,\tau,\sigma) \leq 0$ has not been violated, i.e. the bold green line in Fig. 1.

Fig. 1 also illustrates that condition $\phi(x, T_m, \sigma) < 0$ ensures that maximum solutions are complete, since the solutions to the system have to enter in the red area and have then to enter in the jump set.

As for the periodic time-triggered control case, one has first to prove the well-posedness of this new hybrid dynamical system. This is done in the next proposition.

Proposition 4. *System $\tilde{\mathcal{H}}(f, G, \tilde{\mathcal{C}}, \tilde{\mathcal{D}})$ is well posed.*

The proof is similar to the one of Proposition 1 and is therefore omitted.

The solutions of $\tilde{\mathcal{H}}$ are given in dom(x, τ, σ) provided in (10). As for the time-triggered control implementation, let us now define the set of the particular arcs starting in the origin for $\tilde{\mathcal{H}}$, which are similar to $\mathcal{E}$ for $\mathcal{H}$.

Definition 3. Let us introduce the following set of hybrid arcs, defined as follows:

$$\tilde{\mathcal{E}} = \left\{ \begin{bmatrix} x \\ \tau \\ \sigma \end{bmatrix} \in \mathbb{R}^n \times [0, T_m] \times \mathbb{K} \mid x = [\, I \; 0 \,] e^{\Gamma_\sigma \tau} \begin{bmatrix} 0 \\ 1 \end{bmatrix} \right\}. \tag{36}$$

The set has the same definition as in the periodic case. The only difference is that it only contains the trajectories of the system that are located at $x = 0$ after a jump and that flow until the minimum dwell time T_m is reached. Of course, thanks to the event-triggered control law, these trajectories may continue flowing after the minimum dwell time. However, this set is only defined to understand that the trajectories that starts at $x = 0$ after a jump stay close enough to the operating point and to the attractor defined in the next section.

4.2. Definition of the attractor for event-triggered control

The attractor related to system (5) with an aperiodic sampled-data control implementation, is defined with the same candidate Lyapunov function as for the periodic time-triggered case, i.e.

$$V(x, \tau, \sigma) = \max\{W(x, \tau, \sigma) - 1, 0\}, \tag{37}$$

where W is given in (15) and where we have also kept the same definition for $\mathcal{P}(\tau, \sigma)$ introduced in (16). We recall that matrices Γ_i have been given in (11) and that $\mathcal{P} \succ 0$, which is directly deduced from the definite-positiveness of P. In the sequel, the new compact attractor is

$$\tilde{\mathcal{A}} := \left\{ (x, \tau, \sigma) \in \tilde{\mathcal{C}} \cup \tilde{\mathcal{D}}, \quad V(x, \tau, \sigma) = 0 \right\}. \tag{38}$$

In other words, this attractor is the subset of $\tilde{\mathbb{H}}$, where the solutions to $\tilde{\mathcal{H}}$ satisfy $W(x, \tau, \sigma) \leq 1$ and $\tau < T_M$. We are now in position to state the next theorem.

Theorem 2. *For a given $z_e \in \Omega_e$ and given $T_m, T_M \in \mathbb{R}$, such that, $0 < T_m < T_M$, assume that matrices $0 \prec P \in \mathbb{R}^{n\times n}$, $M = M^\top \in \mathbb{R}^{(n+1)\times(n+1)}$, $h \in \mathbb{R}^n$, $N_i = N_i^\top \in \mathbb{R}^{(n+1)\times(n+1)}$ and parameters $\mu \in (0, 1)$ are the solution to the optimization problem*

$$\min_{P, M, h, N_i, \mu} \quad -\log(\det(P)), \tag{39}$$

$$\text{s.t. } P \succ 0, \quad M \succ 0, \quad \Theta_\lambda(T_m) \succeq 0, \tag{40}$$

$$\begin{bmatrix} \Psi_i(T_m) + (N_\lambda - N_i) + e^{\Gamma_i^\top T_m} M e^{\Gamma_i T_m} - \begin{bmatrix} 0 & 0 \\ * & \mu \end{bmatrix} & \mu \begin{bmatrix} P \\ h^\top \end{bmatrix} \\ * & -\mu P \end{bmatrix} \prec 0,$$

$$\forall i \in \mathbb{K}, \tag{41}$$

where $\Psi_i(T_m)$ and $\Theta_\lambda(T_m)$ are given in (22) and (21), respectively, with T_m replacing T and with $\lambda \in \Lambda$ related to z_e satisfying Assumption 3. Then, the following control law, given by

$$u(x, \tau, \sigma) \in \underset{j\in\mathbb{K}}{\operatorname{argmin}} \begin{bmatrix} x \\ 1 \end{bmatrix}^\top N_j \begin{bmatrix} x \\ 1 \end{bmatrix} \tag{42}$$

with $x := z - z_e$ together with the event-triggering rule

$$\phi(x, \tau, \sigma) = \begin{bmatrix} x \\ 1 \end{bmatrix}^\top \left(\mathcal{P}(0, \sigma) - e^{\Gamma_\sigma^\top (T_m - \tau)} (\mathcal{P}(0, \sigma) + M) e^{\Gamma_\sigma (T_m - \tau)} \right) \begin{bmatrix} x \\ 1 \end{bmatrix} \tag{43}$$

ensures that map G is locally bounded and outer semi-continuous and the following statements hold for hybrid system (31)–(32):

(i) *attractor $\tilde{\mathcal{A}}$ defined in (38) is UGAS and*

(ii) *set $\tilde{\mathcal{E}}$ defined in (36) is included in attractor $\tilde{\mathcal{A}}$.* □

Proof 5. Consider the solution of the optimization described in Theorem 2, for a given minimum dwell time, T_m and a maximum dwell time, T_M, which is selected arbitrarily with the only constraint that $T_M > T_m$. Then, we proceed with the proof of items (i) and (ii).

Proof of (i): The proof of item (i) relies on the application of [33, Theorem 1]. It is easy to see that V presents, as in the previous section, the properties of continuity in $\tilde{\mathcal{C}} \cup \tilde{\mathcal{D}}$, locally Lipschitz near each point in $\tilde{\mathcal{C}} \backslash \tilde{\mathcal{A}}$, positive definiteness with respect to $\tilde{\mathcal{A}}$ in $\tilde{\mathcal{C}} \cup \tilde{\mathcal{D}}$ and radially unbounded.

Now, the next step of the proof is to ensure

$$\langle \nabla V(x,\tau,\sigma), f(x,\sigma)\rangle \leq 0, \quad \forall (x,\tau,\sigma) \in \tilde{\mathcal{C}}\backslash\tilde{\mathcal{A}}. \tag{44}$$

From the definition of the Lyapunov function given in (37), we get

$$\begin{aligned} &\langle \nabla V(x,\tau,\sigma), f(x,\tau,\sigma)\rangle \\ &= \begin{bmatrix} x \\ 1 \end{bmatrix}^\top \left(\dot\tau \tfrac{\partial}{\partial \tau}\mathcal{P}(\tau,\sigma) + \dot\sigma \tfrac{\partial}{\partial \sigma}\mathcal{P}(\tau,\sigma)\right)\begin{bmatrix} x \\ 1 \end{bmatrix} + 2\begin{bmatrix} x \\ 1 \end{bmatrix}^\top \mathcal{P}(\tau,\sigma)\begin{bmatrix} \dot x \\ 0 \end{bmatrix} \\ &= \begin{bmatrix} x \\ 1 \end{bmatrix}^\top (1-\dot\tau)\,\mathrm{He}\left(\mathcal{P}(\tau,\sigma)\Gamma_\sigma\right)\begin{bmatrix} x \\ 1 \end{bmatrix} = 0, \end{aligned} \tag{45}$$

which is guaranteed by the positive definiteness of V in $\tilde{\mathcal{C}}\backslash\tilde{\mathcal{A}}$. The next step consists in establishing the following condition during jumps

$$\Delta V(x,\tau,\sigma) := \max_{\tilde g \in G(x,\tau,\sigma)\cap(\tilde{\mathcal{C}}\cup\tilde{\mathcal{D}})} V(\tilde g) - V(x,\tau,\sigma) < 0, \quad \forall (x,\tau,\sigma) \in \tilde{\mathcal{D}}\setminus\tilde{\mathcal{A}}. \tag{46}$$

Let us first note that, if the first term of the right hand side is 0 (i.e. $\tilde g \in \tilde{\mathcal{A}}$), then, the negativity of the previous equation is trivially satisfied. If not, we have, from the definition of V in (37),

$$\begin{aligned} \Delta V(x,\tau,\sigma) &= W(x^+,0,\sigma^+) - W(x,T,\sigma) \\ &= \begin{bmatrix} x \\ 1 \end{bmatrix}^\top \left(\mathcal{P}(0,\sigma) - e^{-\Gamma_\sigma^\top \tau}\mathcal{P}(0,\sigma)e^{-\Gamma_\sigma\tau}\right)\begin{bmatrix} x \\ 1 \end{bmatrix} \\ &= \begin{bmatrix} x \\ 1 \end{bmatrix}^\top e^{-\Gamma_\sigma^\top\tau}\left(e^{\Gamma_\sigma^\top T_m}\left(\mathcal{P}(0,\sigma)+M\right)e^{\Gamma_\sigma T_m} - \mathcal{P}(0,\sigma)\right)e^{-\Gamma_\sigma\tau}\begin{bmatrix} x \\ 1 \end{bmatrix} \\ &\quad + \begin{bmatrix} x \\ 1 \end{bmatrix}^\top \left(\mathcal{P}(0,\sigma) - e^{\Gamma_\sigma^\top(T_m-\tau)}(\mathcal{P}(0,\sigma)+M)e^{\Gamma_\sigma(T_m-\tau)}\right)\begin{bmatrix} x \\ 1 \end{bmatrix}. \end{aligned}$$

Recalling the procedure presented in the proof of the periodic time-triggered control case in Eq. (26) and identifying the event-triggering rule ϕ given in (43), the previous expression can be rewritten as follows

$$\Delta V(x,\tau,\sigma) = \begin{bmatrix} x \\ 1 \end{bmatrix}^\top e^{-\Gamma_\sigma^\top\tau}\left(\Psi_\sigma(T_m) + e^{\Gamma_\sigma^\top T_m}Me^{\Gamma_\sigma T_m}\right)e^{-\Gamma_\sigma\tau}\begin{bmatrix} x \\ 1 \end{bmatrix} + \phi(x,\tau,\sigma)$$

where matrix $\Psi_\sigma(T_m)$ is given in (22) with $T = T_m$. Following the same techniques as for the periodic time-triggered control case, we note that

$$\begin{aligned} \Delta V(x,\tau,\sigma) &= \begin{bmatrix} x \\ 1 \end{bmatrix}^\top e^{-\Gamma_\sigma^\top\tau}\bar\Phi_\sigma(T_m)e^{-\Gamma_\sigma\tau}\begin{bmatrix} x \\ 1 \end{bmatrix} + \phi(x,\tau,\sigma) \\ &\quad - \begin{bmatrix} x \\ 1 \end{bmatrix}^\top e^{-\Gamma_\sigma^\top\tau}\left(N_\lambda - N_\sigma\right)e^{-\Gamma_\sigma\tau}\begin{bmatrix} x \\ 1 \end{bmatrix} \\ &\quad - \mu\begin{bmatrix} x \\ 1 \end{bmatrix}^\top e^{-\Gamma_\sigma^\top\tau}\begin{bmatrix} P & h \\ h^\top & h^\top P^{-1}h - 1 \end{bmatrix}e^{-\Gamma_\sigma\tau}\begin{bmatrix} x \\ 1 \end{bmatrix}. \end{aligned}$$

where we have introduced the notation

$$\bar\Phi_i(T_m) = \Psi_\sigma(T) + e^{\Gamma_i^\top T_m}Me^{\Gamma_i T_m} + N_\lambda - N_i + \mu\begin{bmatrix} P & h \\ h^\top & h^\top P^{-1}h - 1 \end{bmatrix}, \quad \forall i \in \mathbb{K}.$$

One may recognize, in the second line of the previous expression of ΔV, the expression of Σ_σ given in (28), and the definition of the Lyapunov function in the third line. This brings us to rewrite the previous expression as follows,

$$\begin{aligned} \Delta V(x,\tau,\sigma) &= \begin{bmatrix} x \\ 1 \end{bmatrix}^\top e^{-\Gamma_\sigma^\top\tau}\bar\Phi_\sigma(T_m)e^{-\Gamma_\sigma\tau}\begin{bmatrix} x \\ 1 \end{bmatrix} \\ &\quad - \Sigma_\sigma(x,\tau,\sigma) - \mu\left(W(x,\tau,\sigma) - 1\right) + \phi(x,\tau,\sigma). \end{aligned}$$

Hence, we are now ready to ensure the negative definiteness of ΔV. Using a Schur complement to (41), we can guaranty that $\bar\Phi_\sigma(T_m) \prec 0$ holds for any $\sigma \in \mathbb{K}$. Consequently, the first term of the previous expression is negative definite. The second term is negative because of the control law and the third term is also negative since, as for the periodic time-triggered case, this term refers to the assumption that the state, just before a jump occurs, is outside of the attractor. The previous discussion means that there exists a sufficiently small $\varepsilon > 0$ such that

$$\Delta V(x,\tau,\sigma) \leq -\varepsilon \left\| \begin{smallmatrix} x \\ \tau \\ \sigma \end{smallmatrix} \right\|^2 + \phi(x,\tau,\sigma). \tag{47}$$

Note that this last inequality is made possible since τ is bounded by T_M. According to the definition of the jump set in (34), two cases may occur.

Case I (x, τ, σ) is in $\mathcal{D}_{T_m} \cap \mathcal{D}_e$. This means that $\tau \geq T_m$ and $\phi(x, \tau, \sigma) = 0$. Then, it is clear that $\Delta V(x, \tau, \sigma) \leq -\varepsilon \left\| \begin{smallmatrix} x \\ \tau \\ \sigma \end{smallmatrix} \right\|^2$.

Case II (x, τ, σ) is in $\mathcal{D}_{T_M}$. This means that $\tau = T_M$ and $\phi(x, \tau, \sigma) \leq 0$, then (47) holds.

Now, we need to prove the invariance of $\tilde{\mathcal{A}}$ for $(x, \tau, \sigma) \in \tilde{\mathcal{H}}$. From (45), we have $\langle \nabla \tilde{V}(x, \tau, \sigma), \tilde{f}(x, \tau, \sigma) \rangle = 0$, for all (x, τ, σ) in $(\tilde{\mathcal{C}} \cap \tilde{\mathcal{A}}) \subset \tilde{\mathcal{A}}$, which ensures that the solution in the attractor remains in it during flows.

We now need to prove that the solution to $\tilde{\mathcal{H}}$ that enters into $\tilde{\mathcal{A}}$ remains in the attractor during jumps, i.e. $G(\tilde{\mathcal{D}} \cap \tilde{\mathcal{A}}) \subset \tilde{\mathcal{A}}$. To do so, let us note that condition (20) can be rewritten as follows

$$\begin{array}{rcl} W(x, 0, \sigma^+) & = & W(x, \tau, \sigma) + \Delta W(x, \tau, \sigma) \\ & = & W(x, \tau, \sigma) + \begin{bmatrix} x \\ 1 \end{bmatrix}^\top e^{-\Gamma_\sigma^\top \tau} \Phi_\sigma(T_m) e^{-\Gamma_\sigma \tau} \begin{bmatrix} x \\ 1 \end{bmatrix} \\ & & - \Sigma_\sigma(x, \tau, \sigma) - \mu \left(W(x, \tau, \sigma) - 1 \right) + \phi(x, \tau, \sigma) \\ & \leq & W(x, \tau, \sigma) - \mu (W(x, \tau, \sigma) - 1) \\ & = & (1 - \mu)(W(x, \tau, \sigma) - 1) + 1. \end{array}$$

Then, for any $(x, \tau, \sigma) \in \tilde{\mathcal{A}}$, for which we have $W(x, \tau, \sigma) - 1 < 0$, the assumption $\mu \in (0, 1)$ that guaranties $W(x, 0, \sigma^+) < 1$ holds. From its definition, this also means that $V(x, 0, \sigma^+) = 0$. In other words, the previous statement allows us stating which was to be demonstrated, i.e.

$$\Delta V(x, \tau, \sigma) = 0, \quad \forall (x, \tau, \sigma) \in \tilde{\mathcal{D}} \cap \tilde{\mathcal{A}}.$$

As for the periodic time-triggered case, the last step of the proof is to ensure that no complete solution, that are not in $\mathcal{A}$, keeps constant. This is ensured by the fact that the solution will eventually jump after, at most, T_M unit of ordinary time. Since, thanks to the previous developments, we have shown that at each jump, the increment of the Lyapunov function is strictly decreasing.

Proof of (ii): The proof of $\tilde{\mathcal{E}} \subset \tilde{\mathcal{A}}$ follows from the proof of (ii) in Proof 2. Recall that the set $\tilde{\mathcal{E}}$ is defined by all solutions that start at $x = 0$ just after a jump and evolve in $\tau \in [0, T_m]$. It is easy to see that if matrix inequalities (41) are satisfied, then the particular solutions in $\tilde{\mathcal{E}}$ are in $\tilde{\mathcal{A}}$, as done in the proof of Theorem 1.

As noted in Remark 2, the non-convex optimization problem (39)–(41) is transformed in convex, pre-selecting parameter μ by a line-search routine algorithm.

A similar statement as the one in Proposition 2 for Theorem 1 can be formulated for Theorem 2, where a necessary condition for the feasibility of (41) is the existence of weighting parameters $\lambda_i \geq 0$ such that $\sum_{i \in \mathbb{K}} \lambda_i = 1$ and $\sum_{i \in \mathbb{K}} \lambda_i e^{A_i T_m}$ is Schur stable. Moreover, if there also exist $\lambda_i \geq 0$ such that $\sum_{i \in \mathbb{K}} \lambda_i = 1$ and $\sum_{i \in \mathbb{K}} \lambda_i A_i$ is Hurwitz stable, then the previous matrix inequalities will be feasible for a sufficiently small T_m. The proofs of these two statements are omitted because there are direct from the ones of Propositions 2 and 3.

5. Numerical validation

In this section, we take the system driven by (1) composed by three functioning modes:

$$\begin{array}{lll} A_1 = \begin{bmatrix} 0 & 0.5 \\ 0 & -1 \end{bmatrix}, & \mathcal{B}_1 = & \begin{bmatrix} 1 \\ 0.5 \end{bmatrix}, \\ A_2 = \begin{bmatrix} 0.1 & 0 \\ -1 & -1 \end{bmatrix}, & \mathcal{B}_2 = & \begin{bmatrix} -1 \\ -0.5 \end{bmatrix}, \\ A_3 = \begin{bmatrix} 0 & 1 \\ -1 & 0 \end{bmatrix}, & \mathcal{B}_3 = & \begin{bmatrix} 0 \\ 2 \end{bmatrix}. \end{array} \tag{48}$$

The desired operating point is $z_e = [0.1 \;\; 0.2]^T$ associated with $\lambda = [0.40 \;\; 0.47 \;\; 0.13]$ belongs to Ω_e. Note that the each functioning mode is instable.

We consider the following switching times for the time-triggered control (2) as well as the minimum dwell times for the event-triggered control (3): $T = T_m = 0.25$, 0.5 and 1s. The maximum dwell-time is arbitrarily selected as $T_M = 100$s. As mentioned in Remark 2, numerical results have been obtained on MATLAB by performing a line-search algorithm on parameter $\mu \in (0, 1)$, and then solving the resulting convex optimization using the CVX sdp solver [36].

We first stress that the optimal solutions obtained from both Theorems 1 and 2 are the same given in Table 1, even though the conditions are different, because of matrix M in the event-triggered case. Looking at the numerical values, matrix M is of order 10^{-10} in all cases. Therefore, comparatively to the values of P given in Table 1, its influence can be neglected. This can be expected from the conditions since the only constraint on M is to be positive definite.

Table 1
Numerical results for the time-triggered control and for the event-triggered control with $T = T_m$ in the hybrid dynamical formulation (6)–(7) and (31)–(32), respectively.

	μ	$\det(P)^{\frac{1}{2}}$	P	h
T = 0.1	0.03	1.03	$\begin{bmatrix} 1.5528 & 0.6818 \\ 0.6818 & 0.9055 \end{bmatrix}$	$\begin{bmatrix} -0.1848 \\ -0.0723 \end{bmatrix}$
T = 0.6	0.09	11.21	$\begin{bmatrix} 0.1600 & 0.0473 \\ 0.0473 & 0.0637 \end{bmatrix}$	$\begin{bmatrix} -0.004 \\ -0.002 \end{bmatrix}$
T = 1	0.09	20.56	$\begin{bmatrix} -0.0010 & -0.0001 \\ -0.0001 & 0.0014 \end{bmatrix}$	$\begin{bmatrix} -0.0043 \\ -0.0016 \end{bmatrix}$

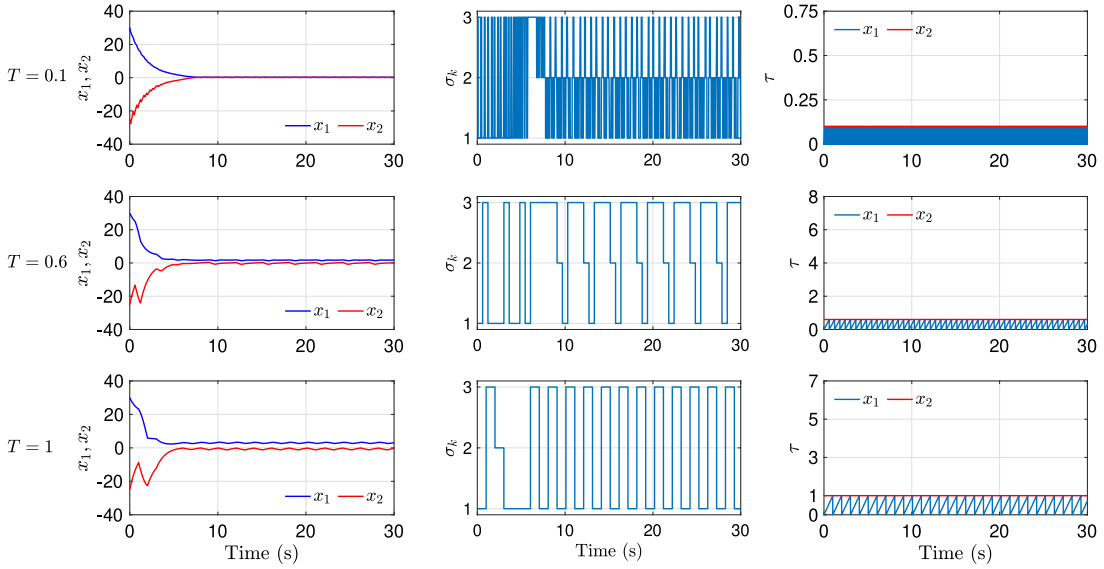

Fig. 2. Simulation results of switched affine system (1), (48) with the periodic time-triggered control for three different values of T, from top to bottom. From left to right, the figure shows the evolution of the state variables (x_1, x_2), the control input σ and the timer τ.

5.1. Comments on the periodic time-triggered control

On the one hand, some simulations are performed when the periodic time-triggered control law given in (2) is applied to system (1) via the hybrid dynamical system (6)–(7), with the parameters computed from the optimization problem given in Theorem 1. Fig. 2 shows the time evolution of the state x, the control input σ and the timer τ. Note in the second column of Fig. 2, that the reached operating point and its associated weighting vector are different to the pair (z_e, λ). Indeed, the system converges asymptotically to a neighborhood of the origin, evolving in the hybrid time domain (10), as hybrid arcs. The last column shows timer τ bounded by T, driving to periodic-time switching.

Fig. 3, shows, in the first column, the convergence of the solutions to $\mathcal{A}$, which is illustrated through the graph of $W(x, \tau, \sigma)$. Indeed, the solutions enter into $\mathcal{A}$ when $W(x, \tau, \sigma)$ is lower than 1. In the second column, we highlight more insights on the attractor. To do so, let us introduce the following function $\mathcal{F}$ from $[0, T] \times \mathbb{K}$ to $\mathbb{R}^n$, which represents the boundary of the attractor $\mathcal{A}$ projected on the state space x. More formally, let us define $\mathcal{F}$ as follows

$$\mathcal{F}(\tau, \sigma) := \{x \in \mathbb{R}^n, \quad W(x, \tau, \sigma) = 1\}, \quad \forall (\tau, \sigma) \in [0, T] \times \mathbb{K}.$$

It is worth noting that the graph of $\mathcal{F}(\tau, \sigma)$ draws, for each value of τ and σ, an ellipsoid. It can be seen that the increasing of T implies an expected increase of the volume of $\mathcal{F}(\tau, \sigma)$ independently on τ and σ. This increase of $\mathcal{A}$ is also appreciated in Table 1, which provides an estimation of the volume of the ellipse drawn by the attractor when $\tau = 0$ (and independent of σ), which is proportional to $\det(P)^{-\frac{1}{2}}$. It is noted as the origin remains in the interior of $\mathcal{A}$.

5.2. Comments on the aperiodic event-triggered control

The same simulation setup has been considered in the aperiodic event-triggered case. Similarly to the time-triggered periodic case, Fig. 4 shows the state evolutions, when the event-triggered control (3) is applied to system (1), via the hybrid dynamical system (31)–(32) with three a priori selected minimum dwell times $T_m = 0.1$, 0.6 and 1. It is appreciated as

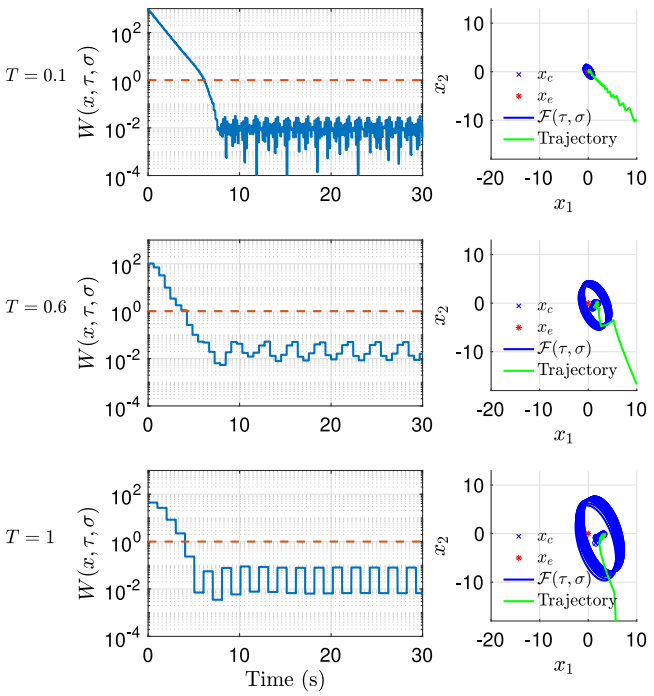

Fig. 3. Simulation results of switched affine system (1), (48) with the periodic time-triggered control for three different values of T, from top to bottom. From left to right, the figure shows the function $W(x, \tau, \sigma)$ (in a logarithmic scale), with respect to time and the second column shows the trajectories of the state space x and the projection of $\mathcal{A}$ in x, i.e. $\mathcal{F}(\tau, \sigma)$.

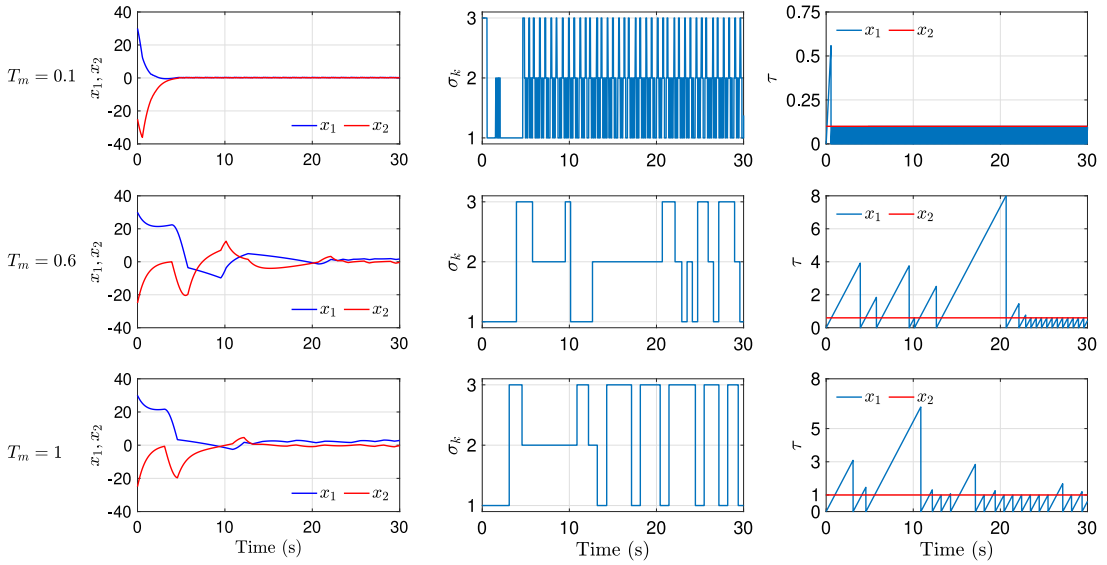

Fig. 4. Simulation results of switched affine system (1), (48) with the aperiodic time-triggered control for three different values of T_m, from top to bottom. From left to right, the figure shows the evolution of the state variables (x_1, x_2), the control input σ and the timer τ.

the timer, τ, generates an aperiodic switching rule between the minimum dwell time T_m and and the maximum dwell time T_M selected arbitrarily as 100.

Comparing the simulation results of Fig. 2 with respect to Fig. 4, which were performed for the same initial conditions, we first remark that the solutions to the systems also converge in a neighborhood of the origin. However, one can also note that the transient period is larger in the event-triggered case compared to the time-triggered one. We can see in the last column of the figure that the timer reaches a periodic behavior once the solutions are close to the operating point. Before that, we can see in these simulations that the solutions to the event-triggered controller are able to flow during

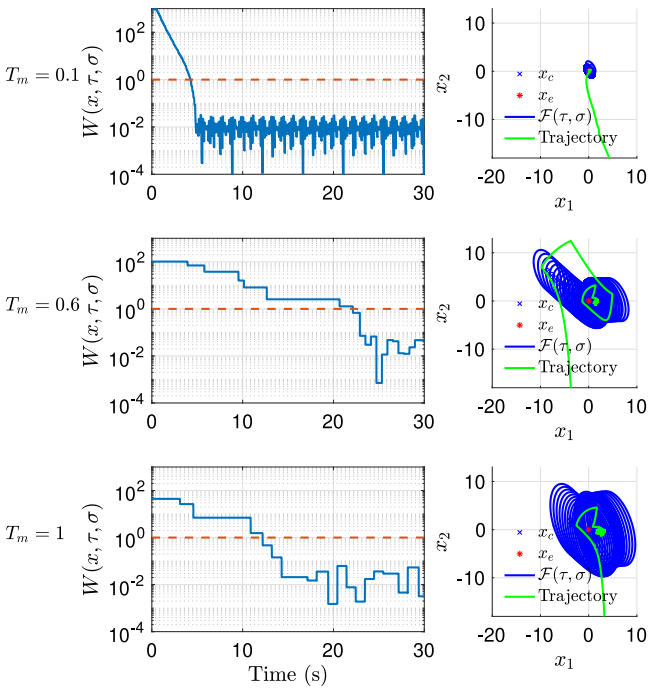

Fig. 5. Simulation results of switched affine system (1), (48) with the aperiodic time-triggered control for three different values of T_m, from top to bottom. From left to right, the figure shows the function $W(x,\tau,\sigma)$ (in a logarithmic scale), with respect to time and the second column shows the trajectories of the state space x and the projection of $\tilde{\mathcal{A}}$ in x.

a notable while (up to 8 units of ordinary time). Therefore, the event-triggered control law is able to reduce the number of control updates compared to the periodic time-triggered case.

Fig. 5 depicts the evolution of $W(x,\tau,\sigma)$ (first column) and the projection of $\tilde{\mathcal{A}}$ into the space x (in the second column). While the optimization problem presented in both theorems delivers the same values, it is emphasized the fact that the timer reaches larger values than the minimum dwell time. This leads to notable differences when plotting the projection of attractor $\tilde{\mathcal{A}}$ (see Fig. 5). Indeed the graphs of $\mathcal{F}(\tau,\sigma)$ for each values of the minimum dwell time T_m presents larger variations compared to the periodic case. However, since the simulations show that the timer seems to converge to a periodic behavior of period T_m, the projections of the attractor in the steady state in both time- and event-triggered converge to the same region.

5.3. Fair comparison between both approaches

When comparing the solutions to the time- and event-triggered controller, it seems that the best performance is achieved by the periodic time-triggered. Indeed, for this set of simulations, the transient of the time-triggered case are shorter than the ones of the event-triggered case, when comparing the solutions with $T = T_m$. However, this comparison is not really fair, since in the periodic solutions requires more control actions than the aperiodic one.

In order to provide a more accurate comparison, let us focus on the solution of the event-triggered case with $T_m = 0.6$. The triggering rule generates 19 events corresponding to a change of mode over a simulation of 30s. Therefore, an equivalent periodic control for this simulation would require to select $T = 30/19$, for which no solution to the optimization problem of Theorem 1 can be found. However, a solution has been obtained for a slightly lower value $T = 1.5$. Fig. 6 now illustrates a fair comparison where the solution to the periodic time-triggered controller with $T = 0.6$ and 1.5 and to the event-triggered controller with $T_m = 0.6$ are presented. Indeed, the two simulations at the bottom of the figure have the same number of control updates. Even though the transient of the periodic solution is shorter than the aperiodic one, the solution to the periodic case has a larger chattering around the operating point compared to the aperiodic case. Moreover, the guarantees of the periodic controller with $T = 1.5$ are much worse than the aperiodic one as shown in Fig. 7, where the projection of the attractor is way much larger than the aperiodic case. Therefore, in light of the previous comments, the event-triggering controller has the merit to reduce the number of control updates while keeping the same guarantees on the size of the attractor, but at the price of reducing the performance during the transient phase.

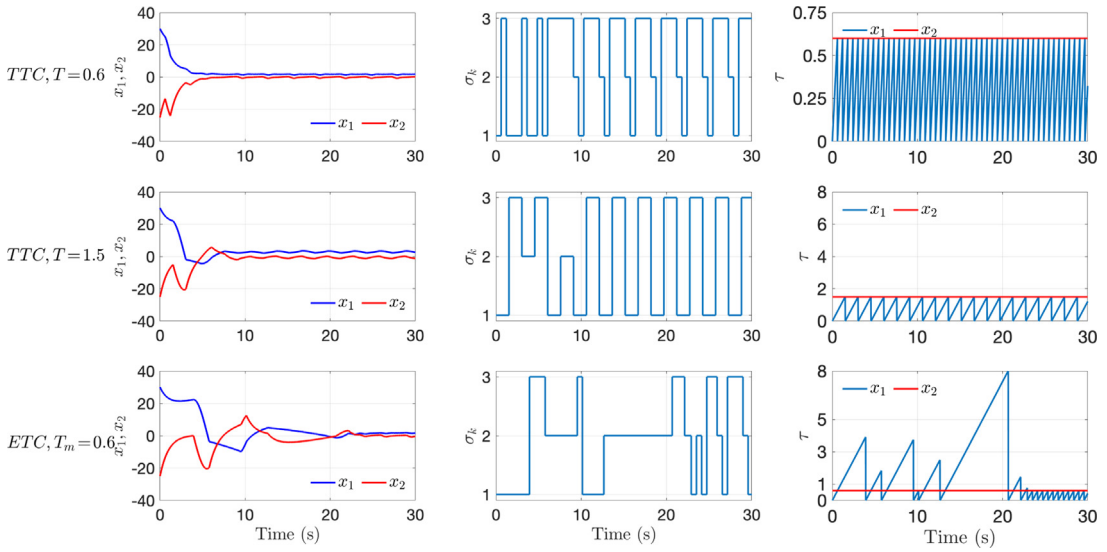

Fig. 6. Simulations presenting the evolution of the state x (left), the selected mode σ (middle) and the timer τ (right) for two time-triggered controller (TTC) with $T = 0.6$ and 1.5 and for the event-triggered case (ETC) with $T_m = 0.6$.

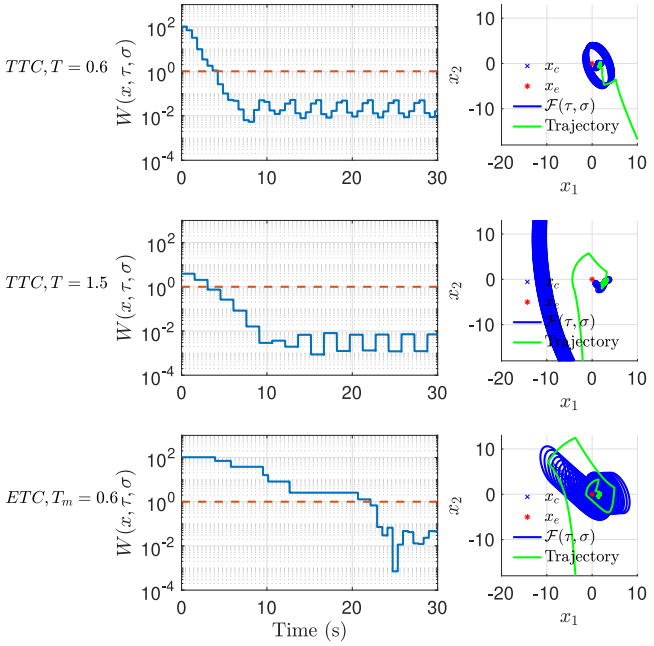

Fig. 7. Simulations presenting the evolution of $W(x, \tau, \sigma)$ (left) and the solutions to the system in the phase plan (right) for two time-triggered controller (TTC) with $T = 0.6$ and 1.5 and for the event-triggered case (ETC) with $T_m = 0.6$.

6. Conclusions and perspectives

This work presents a switching controller for affine systems, defined by continuous-time and discrete-time dynamics, when the input signal is periodically or aperiodically updated. The main result presented here provides a simple control architecture, which is not structured by the system matrices nor the Lyapunov matrix. It is proven UGAS of a compact attractor defined in the hybrid state space (x, τ, σ) and the practical asymptotic stability of the operating point $z_e = z - x$. A deep discussions has been proposed in the numerical application sections and shows the advantages and drawbacks of each control strategies. In future work, we aim at exploiting this framework to ensure the robustness of the system with respect to parameter variations and to jitter.

CRediT authorship contribution statement

Carolina Albea: Conceptualization, Data curation, Formal analysis, Funding acquisition, Investigation, Methodology, Project administration, Resources, Supervision, Validation, Visualization, Writing - original draft, Writing - review & editing. **Alexandre Seuret:** Conceptualization, Data curation, Formal analysis, Investigation, Methodology, Project administration, Resources, Supervision, Validation, Visualization, Writing - original draft, Writing - review & editing.

Declaration of competing interest

The authors declare that they have no known competing financial interests or personal relationships that could have appeared to influence the work reported in this paper.

Acknowledgments

This work has been partially funded by the Agence Nationale de la Recherche (ANR)France under Grant ANR-18-CE40-0022-01 and by the Agencia Estatae Investigación (AEI)-Spain under Grant PID2019-105890RJ-100.

References

[1] D. Liberzon, Switching in Systems and Control, Springer Science & Business Media, 2012.
[2] H. Sira-Ramírez, R. Silva-Ortigoza, Control Design Techniques in Power Electronics Devices, Springer Science & Business Media, 2006.
[3] T. Theunisse, J. Chai, R. Sanfelice, W. Heemels, Robust global stabilization of the dc-dc boost converter via hybrid control, IEEE Trans. Circuits Syst. I: Regul. Papers 62 (4) (2015) 1052–1061.
[4] F. Parise, M.E. Valcher, J. Lygeros, Computing the projected reachable set of stochastic biochemical reaction networks modelled by switched affine systems, IEEE Trans. Automat. Control 63 (11) (2018) 3719–3734.
[5] B. Oh, J. Jeong, J. Suk, S. Kim, Design of a control system for an organic flight array based on a neural network controller, Int. J. Aerosp. Eng. (2018).
[6] M. Hajiahmadi, B. De Schutter, H. Hellendoorn, Robust h-infty switching control techniques for switched nonlinear systems with application to urban traffic control, Internat. J. Robust Nonlinear Control 26 (6) (2016) 1286–1306.
[7] S. Pettersson, B. Lennartson, Stabilization of hybrid systems using a min-projection strategy 1 (2001) 223–228.
[8] C. Seatzu, A. Corona, D. Giua, A. Bemporad, Optimal control of continuous-time switched affine systems, IEEE Trans. Automat. Control 51 (5) (2006) 726–741.
[9] C. Albea-Sanchez, G. Garcia, L. Zaccarian, Hybrid dynamic modeling and control of switched affine systems: application to dc-dc converters (2015) 2264–2269.
[10] G. Deaecto, J. Geromel, F. Garcia, J. Pomilio, Switched affine systems control design with application to DC–DC converters, IET Control Theory Appl. 4 (7) (2010) 1201–1210.
[11] L. Egidio, H. Daiha, G. Deaecto, J. Geromel, DC motor speed control via buck-boost converter through a state dependent limited frequency switching rule (2017) 2072–2077.
[12] A. Sferlazza, C. Albea-Sanchez, L. Martínez-Salamero, G. Garcia, C. Alonso, Min-type control strategy of a DC-dc synchronous boost converter, IEEE Trans. Ind. Electron. 67 (4) (2019) 3167–3179.
[13] Y. Lu, W. Zhang, A piecewise smooth control-lyapunov function framework for switching stabilization, Automatica 76 (2017) 258–265.
[14] J. Buisson, P. Richard, H. Cormerais, On the stabilisation of switching electrical power converters 3414 (2005) 184–197.
[15] M. Senesky, G. Eirea, T. Koo, Hybrid modelling and control of power electronics 2623 (2003) 450–465.
[16] C. Albea-Sanchez, G. Garcia, S. Hadjeras, W. Heemels, L. Zaccarian, Practical stabilization of switched affine systems with dwell-time guarantees, IEEE Trans. Automat. Control 64 (11) (2019) 4811–4817.
[17] P. Colaneri, J.C. Geromel, A. Astolfi, Stabilization of continuous-time switched nonlinear systems, Systems Control Lett. 57 (1) (2008) 95–103.
[18] J. Liu, X. Liu, W. Xie, On.the. (h, On the (h 0, h)-stabilization of switched nonlinear systems via state-dependent switching rule, Appl. Math. Comput. 217 (5) (2010) 2067–2083.
[19] M. Kumar, R. Gupta, Sampled time domain analysis of digital pulse width modulation for feedback controlled converters, IET Circuits Devices Syst. 10 (6) (2016) 481–491.
[20] X. Sun, X. Li, Y. Shen, B. Wang, X. Guo, Dual-bridge LLC resonant converter with fixed-frequency PWM control for wide input applications, IEEE Trans. Power Electron. 32 (1) (2017) 69–80.
[21] F. Bernelli-Zazzera, P. Mantegazza, Pulse-width equivalent to pulse-amplitude discrete control of linear systems, J. Guid. Control Dyn. 15 (2) (1992) 461–467.
[22] S. Ibrir, W. Xie, C. Su, Observer-based control of discrete-time lipschitzian non-linear systems: application to one-link flexible joint robot, Internat. J. Control 78 (6) (2005) 385–395.
[23] P. Nino-Suarez, E. Aranda-Bricaire, M. Velasco-Villa, Discrete-time sliding mode path-tracking control for a wheeled mobile robot (2006) 3052–3057.
[24] P. Hauroigne, P. Riedinger, C. Iung, Switched affine systems using sampled-data controllers: Robust and guaranteed stabilisation, IEEE Trans. Automat. Control 56 (12) (2011) 2929–2935.
[25] G. Deaecto, J. Geromel, Stability analysis and control design of discrete-time switched affine systems, IEEE Trans. Automat. Control 62 (8) (2017) 4058–4065.
[26] C. Albea Sanchez, A. Ventosa-Cutillas, A. Seuret, F. Gordillo, Robust switching control design for uncertain discrete-time switched affine systems, Int. J. Robust Nonlinear Control (2019) http://dx.doi.org/10.1002/rnc.5158.
[27] R. Goebel, R. Sanfelice, A. Teel, Hybrid Dynamical Systems: modeling, stability, and robustness, Princeton University Press, 2012.
[28] L. Torquati, R. Sanfelice, L. Zaccarian, A hybrid predictive control algorithm for tracking in a single-phase DC-AC inverter (2017) 904–909.
[29] L. Hetel, C. Fiter, H. Omran, A. Seuret, E. Fridman, J.-P. Richard, S.-I. Niculescu, Recent developments on the stability of systems with aperiodic sampling: An overview, Automatica 76 (2017) 309–335.
[30] L. Hetel, E. Fridman, Robust sampled–data control of switched affine systems, IEEE Trans. Automat. Control 58 (11) (2013) 2922–2928.
[31] C. Edwards, Sliding mode control: theory and applications, Vol. 131, 1998.

[32] A. Cutillas, C. Albea Sanchez, A. Seuret, F. Gordillo, Relaxed periodic switching controllers of high-frequency DC-DC converters using the δ-operator formulation (2018) 3433–3438.
[33] A. Seuret, C. Prieur, S. Tarbouriech, A. Teel, L. Zaccarian, A nonsmooth hybrid invariance principle applied to robust event-triggered design, IEEE Trans. Automat. Control 64 (5) (2018) 2061–2068.
[34] C. Briat, Convex conditions for robust stabilization of uncertain switched systems with guaranteed minimum and mode-dependent dwell-time, Systems Control Lett. 78 (2015) 63–72.
[35] J. Jin, J. Ramirez, S. Wee, D. Lee, Y. Kim, N. Gans, A switched-system approach to formation control and heading consensus for multi-robot systems, Intell. Serv. Robot. 11 (2) (2018) 207–224.
[36] M. Grant, S. Boyd, CVX: Matlab software for disciplined convex programming, 2014, version 2.1.